Atmospheric Environment 123 (2015) 357–369

Contents lists available at ScienceDirect

Atmospheric Environment

journal homepage: www.elsevier.com/locate/atmosenv

# A study of vertical distribution patterns of $PM_{2.5}$ concentrations based on ambient monitoring with unmanned aerial vehicles: A case in Hangzhou, China

Zhong-Ren Peng [a, b, *], Dongsheng Wang [a], Zhanyong Wang [a], Ya Gao [a], Sijia Lu [a]

[a] Center for ITS and UAV Applications Research, State Key Laboratory of Ocean Engineering, School of Naval Architecture, Ocean & Civil Engineering, Shanghai Jiao Tong University, Shanghai 200240, China
[b] Department of Urban and Regional Planning, University of Florida, PO Box 115706, Gainesville, FL 32611-5706, USA

## HIGHLIGHTS

- Three-dimensional observations of $PM_{2.5}$ mass are conducted using unmanned aerial vehicle with mobile sensors.
- Vertical profile of $PM_{2.5}$ mass concentrations is characterized with four time periods of four days.
- Relationship between $PM_{2.5}$ mass and meteorological parameters is discussed at 300 m–1000 m altitude.

## ARTICLE INFO

*Article history:*
Received 8 March 2015
Received in revised form
26 October 2015
Accepted 26 October 2015
Available online 30 October 2015

*Keywords:*
Fine particulate matter
Vertical distribution
Meteorological parameters
Unmanned aerial vehicle

## ABSTRACT

Measurements of the vertical distribution of air pollutant concentrations can provide essential information for accurate estimates of the dispersion mechanism of local pollutants between boundary layer and troposphere. This paper reports unique measurements using an unmanned aerial vehicle (UAV) with mobile sensors to collect three-dimensional fine particulate matter ($PM_{2.5}$) mass concentration data on sixteen flights within 1000 m altitude from August, 2014 to December, 2014 in Hangzhou, China.

The study demonstrates the feasibility of UAV with mobile monitoring devices as an effective and flexible means to collect three-dimensional air pollutant concentration data, particularly for monitoring the vertical profile of air pollutants. The experimental results show that in general, the $PM_{2.5}$ concentrations decrease as height increases, with an exception when the air temperature inversion layer appears, and the decrease rate of $PM_{2.5}$ concentrations is larger in the morning than in the afternoon flights. This is a result of the accumulated pollutant emission of human activities during the day and the varied meteorological conditions. At the same horizontal layer, there are fluctuations in $PM_{2.5}$ concentrations during different time periods of the day. The vertical fluctuations of $PM_{2.5}$ concentrations become nearly uniform in two afternoon flights, which is directly related with the extent of atmospheric mixture. Seen from the multiple regression models, the distribution of relative $PM_{2.5}$ concentrations between vertical and ground observations is well characterized and the regression coefficients of four measured factors (i.e., air temperature, relative humidity, air pressure and height) effectively explain their impacts on the vertical distribution patterns. Air temperature and relative humidity are the most influential factors that affect the vertical distribution of $PM_{2.5}$ concentrations.



## 1. Introduction

The rapid economic development with a dramatic growth of energy consumption in China is increasing emissions of air pollutants, which has recently induced a series of environmental issues such as the frequent haze and smog (Zhang et al., 2012; Fu et al., 2013). A lot of researches have been conducted to reveal the underlying patterns and reasons behind these environmental

* Corresponding author. Center for ITS and UAV Applications Research, State Key Laboratory of Ocean Engineering, School of Naval Architecture, Ocean & Civil Engineering, Shanghai Jiao Tong University, Shanghai 200240, China.
*E-mail address:* zrpeng@sjtu.edu.cn (Z.-R. Peng).

http://dx.doi.org/10.1016/j.atmosenv.2015.10.074
1352-2310/

issues, but most of them focused on time series analysis at two-dimensional horizontal scale near urban and regional surface (Chang et al., 2009; Che et al., 2009; Quan et al., 2011). As we know, air pollution is a result of local emissions and three-dimensional atmospheric transport (Ramanathan and Feng, 2009). To be specific, air pollution is a process of the surface-to-air mass exchange, and the generation, transport, accumulation and diffusion of air pollution is determined by the dynamic structure of atmospheric boundary layer (Stull, 1988). Hence, it is of particular importance to study the vertical distribution of air pollutants, which can further uncover the exchange mechanism in the atmosphere between atmospheric boundary layer and troposphere, as well as the interaction of internal and external air pollutants (Li et al., 2010).

Vertical measurements of air pollutants have been carried out by various approaches as reported in the literature. Typically, meteorological tower is used for measuring the vertical distribution of air pollutants. Using a 250 m tower, Han et al. (2009) found that the nocturnal planetary boundary layer (NPBL) ranges from 100 m to 150 m in Tianjin, China, and NPBL height has important effects on air pollutants concentrations. Sun et al. (2009) also measured $SO_2$ concentrations at 4 different levels (8 m, 47 m, 120 m, and 280 m) of the 325-m high meteorological observation tower during extreme pollution episodes in Beijing, and found that the highest concentration of $SO_2$ is at the altitude of about 50 m and weather conditions are the major factors influencing the distribution and variation of $SO_2$ concentrations. Because of a limited height and lack of flexibility, meteorological tower is able to measure air pollutants at near-ground height but misses those in the middle- and high-level of planetary boundary layer (PBL). Consequently, the emergence of mountain measurements has overcome the shortcomings of meteorological tower. For example, Raatikainen et al. (2014) studied the effect of PBL dynamics on aerosol properties at the Indo-Gangetic plains and the foothills of the Himalayas where there is a 2000m altitude difference, and concluded that aerosol concentrations at the foothill site are correlated with the average PBL height and a contribution of air mass transport from the plains can occur together with the favorable synoptic scale circulation. Ou-Yang et al. (2014) found the distinct seasonal and diurnal patterns of CO concentrations based on 5-year CO measurements at a mountain-top station with an elevation of 2862 m above mean sea level, and discussed the possible sources. However, mountain measurements are usually conducted at some specific altitude and cannot describe the concentration gradient of air pollutants with the increase of vertical height. Recently, satellite-based remote sensing effectively observes temporal and spatial variation of tropospheric air pollution at multi scales (Streets et al., 2013), but it just integrates the entire column from the surface to the top of the atmosphere as a single layer without vertical gradient measurement (Corrigan et al., 2008). LiDAR is used as a good supplement of surface-based measurement to detect the vertical property of aerosol pollutants, which well reveals the dynamic patterns of vertical structure of aerosol pollutants with time (Chen et al., 2013a; Wang et al., 2014; Ma et al., 2015). The combination of remote sensing and LiDAR technologies is a great improvement to three-dimensional measurement of air pollution at high resolutions, while the measurement accuracy is limited due to lack of sufficient data validation. Sometimes, piloted aircrafts and tethered balloons are directly used to collect continuous data at various altitudes of the atmosphere. Using aircraft, Taubman et al. (2006) studied vertical profiles of $O_3$, CO, $SO_2$ and aerosol over the mid-Atlantic United States; Nunnermacker et al. (2008) measured the mixing ratio of NOx above Mexico City; Geng et al. (2009) explored horizontal and vertical distributions of air pollutants in the Yangtze River Delta region; Berkes et al. (2013) found the low-level wind speed enhanced transport and mixing of CO, $CO_2$, $O_3$ and particle number concentrations from the free troposphere into the PBL; Chen et al. (2013b) concluded that air temperature is the main factor directly causing vertical variation of $O_3$ and NOx mixing ratios at 600–2100 m altitude. Occasionally, tethered balloon is used for detecting vertical profiles of air pollutants. For example, the vertical observations of ozone and VOCs over Mexico City, together with a chemical mass balance model, show that the main contributors to total VOCs and the related ozone formation potential are gasoline vehicle exhaust and liquefied petroleum gas (Wöhrnschimmel et al., 2006). Due to the huge expenses of piloted aircrafts and tethered balloons, these methods are seldom used in research experiments.

As unmanned aerial vehicles (UAVs) have gained popularity for military and civil missions, they have provided a revolutionary new method to monitor ambient air pollutants. An UAV with ambient pollutants sensors is emerging as a new means to produce three-dimensional observations of ambient air pollutants (e.g., Ramanathan et al., 2007, 2008; Ramana et al., 2007; Corrigan et al., 2008). In this study, we carry out UAV campaigns to observe the horizontal and vertical distributions of fine particulate matter ($PM_{2.5}$) with four time periods of the day at the low tropospheric altitude (0–1000 m) in Hangzhou, China. We attempt to verify the technological feasibility of UAV carrying mobile sensor to measure air pollutant concentrations, and to identify the spatial patterns of $PM_{2.5}$ concentrations at three-dimensional scale, as well as to understand the underlying reasons of the vertical distribution patterns.

## 2. Experiments

### 2.1. Experimental design

In order to study the vertical distribution pattern of $PM_{2.5}$ concentrations near the ground (below 1000 m height), an observation experiment based on UAV and mobile sensors was designed around a 4 km*4 km area for collecting data at 300 m–1000 m height (Fig. 1).

A lightweight fixed-wing UAV was used in this experiment. The UAV can lift a 5 kg payload and can fly up to 2 h. The wingspan of the aircraft is about 1.5 m. The UAV can fly autonomously following the flight path designed in advance by the auto pilot system, while it should be launched and recovered by a human pilot.

A suite of mobile sensors were put on the UAV to collect $PM_{2.5}$ and meteorological data. Sidepak AM510 PM Detector with an impactor that provides cuts at 2.5μ is used for getting the mass concentration of $PM_{2.5}$. It records the concentration data every two seconds with a minimum resolution of 1 $\mu g/m^3$. With the built-in sampling pump, air is pumped into a sampling tube through an inlet that towards the UAV tail in order to avoid the effect of variation of the flow rate. As said in our previous studies (Wang et al., 2015a,b), the PM2.5 measurer was calibrated before leaving factory and further estimated with standard methods at outdoor locations in Shanghai, China prior to this field study. Temperature and relative humidity were recorded by HOBO U12 Temp/RH Data Logger, which is fixed outside the fuselage. It records temperature with a resolution of 0.03 °C and records relative humidity with a resolution of 0.03% every two seconds. Columbus V-900 Multifunction GPS Data Logger logs the 3-D location data of the UAV every second.

The UAV was launched by a human pilot, and was switched to autonomous mode when it arrived at a height of 300 m above the ground. Then the UAV flies following the planned path (see Fig. 2). The planned path is like a square, and the UAV flies parallel to the surface of the earth for 3/4 lap and then gains altitude (100 m high per lap). The UAV gains altitude until arrive at 1000 m height above the ground, and then begins to descend back to the ground. The

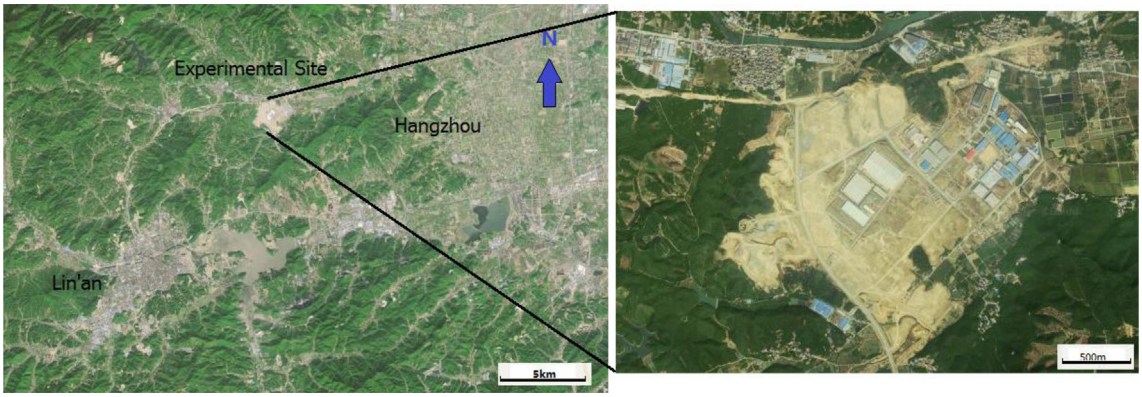


**Fig. 1.** The experimental site: Lin'an, the suburb of the city of Hangzhou, China.

horizontal coverage of the UAV flight is initially 4 km, and decreases as height increases. There is no overlapped point in this flight path, so as to avoid the influence of the emission of the gasoline-fueled UAV. As the flying area may have been influenced by the emission of our UAV, the data during descending process will not be used in this study.

### 2.2. Experimental campaign

The experiments were taken in Lin'an, China, about 40 km from the city of Hangzhou (see Fig. 1). There are no chemical factories or other major polluting sources on the ground near the experimental site. It means that a vertical distribution of air pollutants in the experiments is not influenced by uneven distribution of major ground emission sources.

We have done 6 days and 22 flights of field experiment from August to December in 2014 and have continued experiments every month in 2015. The preliminary data analysis shows remarkable consistency in terms of vertical patterns of $PM_{2.5}$ distribution. To save space, we have chosen to report here only two days of experiments on August 21st and October 11th, 2014. The weather was sunny during the daytime in both days, while the heavy fog appeared in the early morning on August 21st. The wind direction is from the east on August 21st, and from the northeast on October 11th. The wind speed was between 0.5 m/s and 3 m/s near the ground for both days. The background concentrations of $PM_{2.5}$ were extracted from monitored data of Lin'an Environmental Monitoring Centre and the monitors were deployed at a building near the experimental site. A total of four flights were conducted during a day to learn the different patterns in different time periods under different meteorological conditions.

### 2.3. Data processing

All the data for different time interval (6:27–7:07, 10:17–11:07 14:11–15:26, 16:23–17:46 on August 21st and 7:32–8:09, 10:02–10:39, 14:00–14:35, 15:47–16:22 on October 11th) were regularized into 10-s average to reduce sampling errors. For $PM_{2.5}$, the measurement instrument based on light scattering principle can be impacted by relative humidity (McMurry et al., 1996), and thus a correction factor (*CF*) is used to get rid of this error, after which the measurement fits the actual data quite well (Day et al., 2000). *CF* is expressed as follows:

$$CF = 1 + \frac{RH^2}{4(1 - RH)} \quad (1)$$

where RH represents for the relative humidity.

## 3. Results and discussions

### 3.1. Three-dimensional distribution of PM2.5 concentrations

The three-dimensional distribution of $PM_{2.5}$ concentrations is shown in Fig. 2a–d. Generally, the $PM_{2.5}$ concentration decreases as height increases. As for horizontal distribution, there is no obvious difference in all flights as there is no major ground emission source. Furthermore, Fig. 3a and b show the boxplots of the $PM_{2.5}$ concentrations at each height during each flight, and the ground average concentrations corresponding to four flights are presented as well. It can be clearly seen that the $PM_{2.5}$ concentration increases roughly from Flight 1 to Flight 4. The average of the whole $PM_{2.5}$ concentrations is the lowest during Flight 1 but highest during Flight 3. These results coincide with the human activities and atmospheric exchange process during the day. In the early morning, $PM_{2.5}$ concentration is the lowest (Flight 1). With the gradual rise of the sun, radiation and air temperature increases. Human activities cause the emissions of pollutants beginning to accumulate. Because of this, the concentration of $PM_{2.5}$ increases over time until early afternoon. The concentration of $PM_{2.5}$ reaches the peak with the strongest sun radiation (Flight 3). In the afternoon, the sun radiation is weakened, the temperature of atmosphere continues to rise, the local temperature difference and airflow increase, which decreases the concentration of $PM_{2.5}$ (Flight 4) (Fig. 3a).

Compared with the ground level (see Fig. 3a), the vertical level of $PM_{2.5}$ are lower during the flights 2, 3, 4 but higher during Flight 1 on August 21st. In Flight 1, $PM_{2.5}$ concentration increases with the increase of height below 500 m due to thermal inversion layer (at the height of 350–450 m). Typically, air pollutants can transport down to the ground during the night before, which increase the accumulation of pollutants on the ground, but this process is blocked by the inversion layer and thus the $PM_{2.5}$ concentrations are higher above the inversion layer than on the ground.

During Flight 2, the atmospheric boundary layer activity begins to intensify, and then $PM_{2.5}$ concentration at the height of 300–700 m rises rapidly but slowly above 700 m. The Flights 3 and 4 show almost the same pattern due to the similar properties of atmosphere that the atmospheric boundary layer lifts from 500 m to over 1000 m and particles are homogeneously mixed with its vertical movement, which can explain their difference from Flight 1 and Flight 2. In addition, $PM_{2.5}$ concentration varies in a smaller range within 1000 m than that in both Flights 1 and 2, which are directly related with the extent of atmospheric mixing.

The data on October 11th shows similar pattern with data on August 21st (Fig. 3b). $PM_{2.5}$ concentration decreases with the increase of altitude in Flights 2, 3 and 4. During Flight 1, $PM_{2.5}$ concentration increases from 600 m to 800 m due to thermal inversion

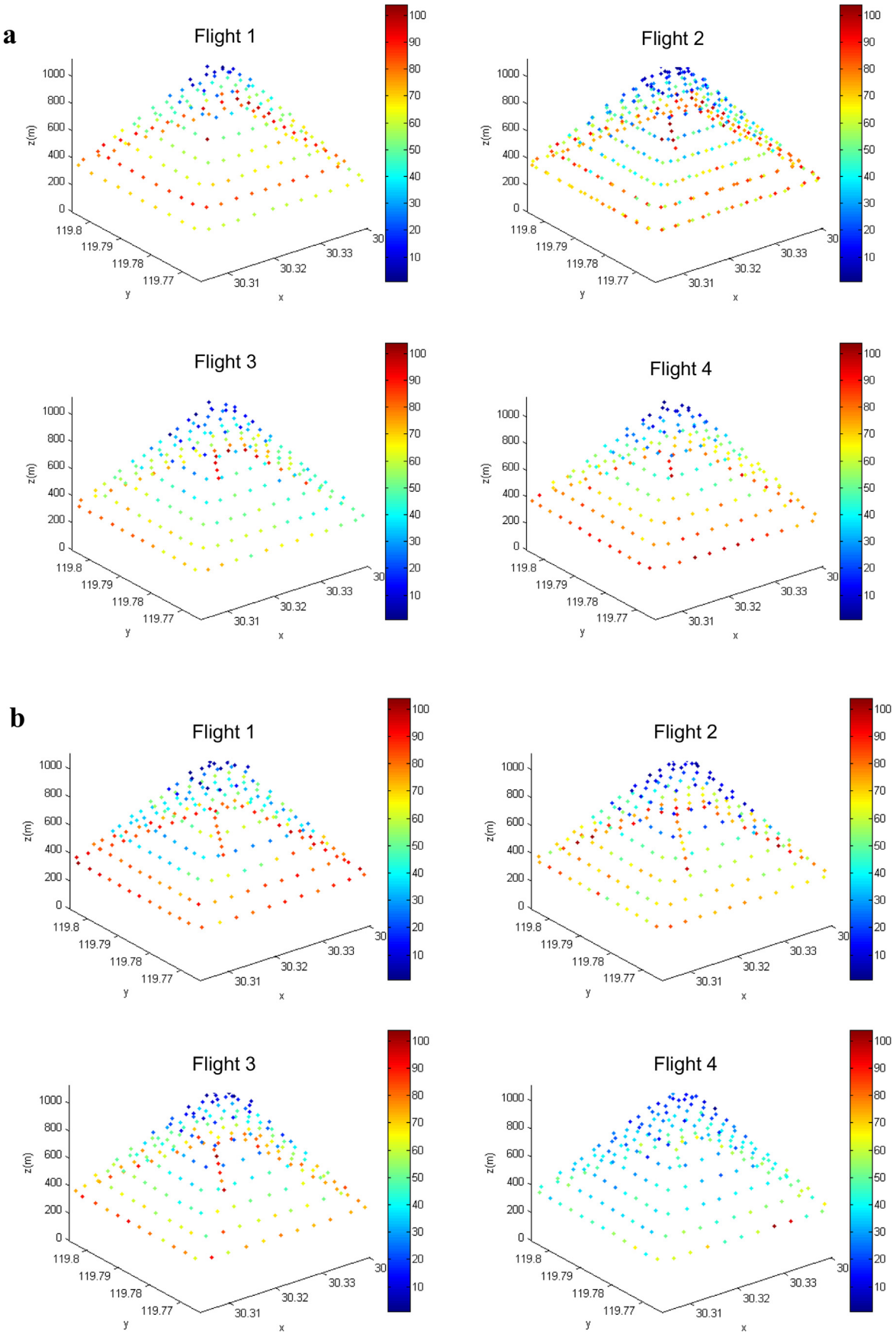


**Fig. 2.** a. Three-dimensional distribution of $PM_{2.5}$ (%) on August 21st. b. Three-dimensional distribution of $PM_{2.5}$ (%) on October 11th. c. Three-dimensional distribution of $PM_{2.5}$ (%) on November 14th. d. Three-dimensional distribution of $PM_{2.5}$ (%) on December 12th (x, y and z axes are represented for latitude (N), longitude (E) and altitude, respectively).

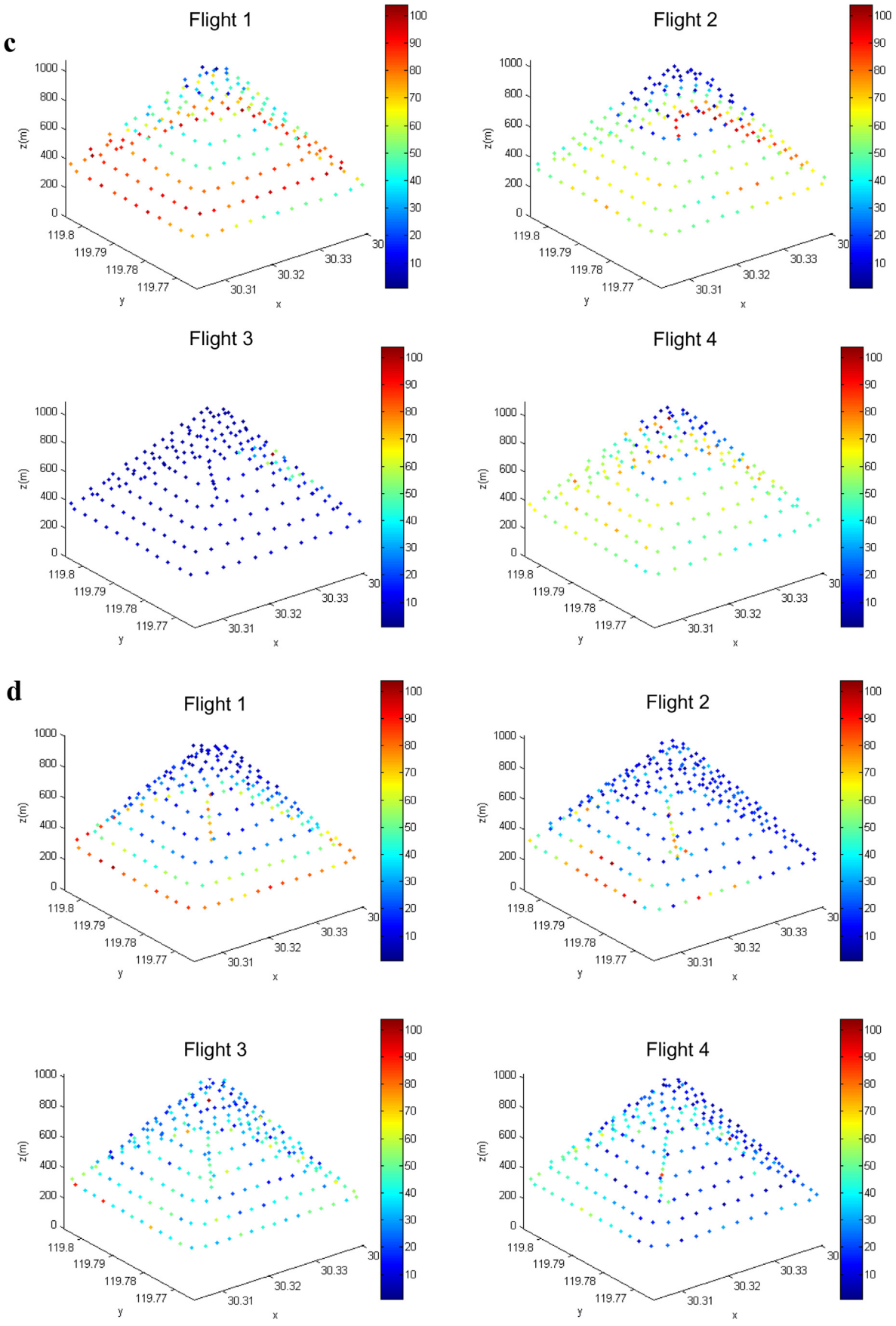


**Fig. 2.** (*continued*).

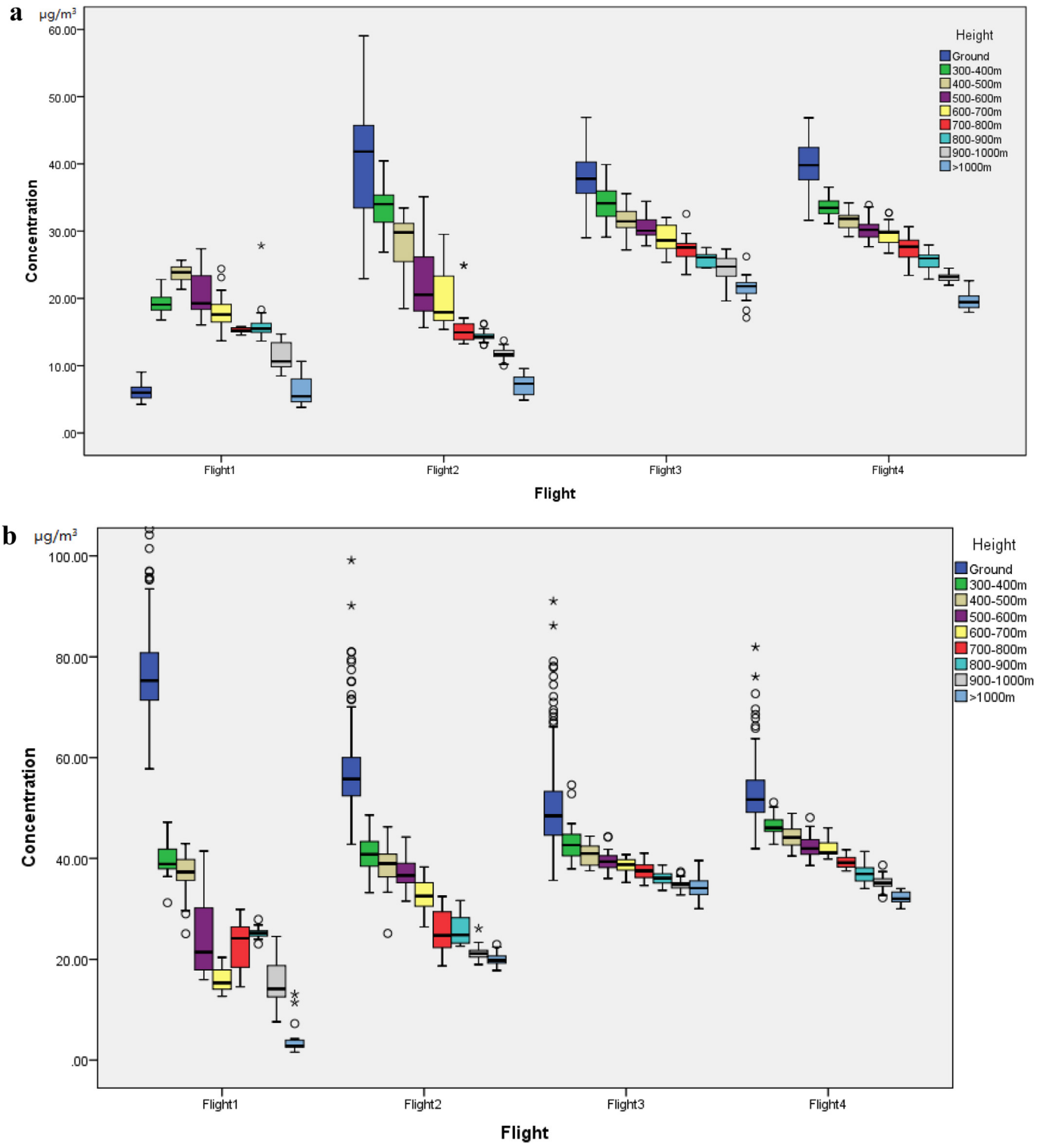


**Fig. 3.** a. Boxplot of $PM_{2.5}$ concentration changes with the increase of altitude on August 21st. b. Boxplot of $PM_{2.5}$ concentration changes with the increase of altitude on October 11th. c. Boxplot of $PM_{2.5}$ concentration changes with the increase of altitude on November 14th. d. Boxplot of $PM_{2.5}$ concentration changes with the increase of altitude on December 12th (Dark blue represents concentrations on the ground corresponding to four flights). (For interpretation of the references to colour in this figure legend, the reader is referred to the web version of this article.)

layer. With the atmospheric boundary layer lifts, the patterns of Flights 2, 3 and 4 on October 11th are the same as that on August 21st.

During the winter days, a certain stratification of the PM2.5 concentrations are shown in the morning (Flight 1 & 2). The $PM_{2.5}$ concentrations in Flight 1 on November 14th (Fig. 4) show two significant aerosol layers between 350 and 450 m and between 800 and 900 m due to shallow inversion layers, which is consistent with the result by the unmanned research aircraft "ALADINA" (Altstädter et al., 2015). A strong surface inversion layer during the morning

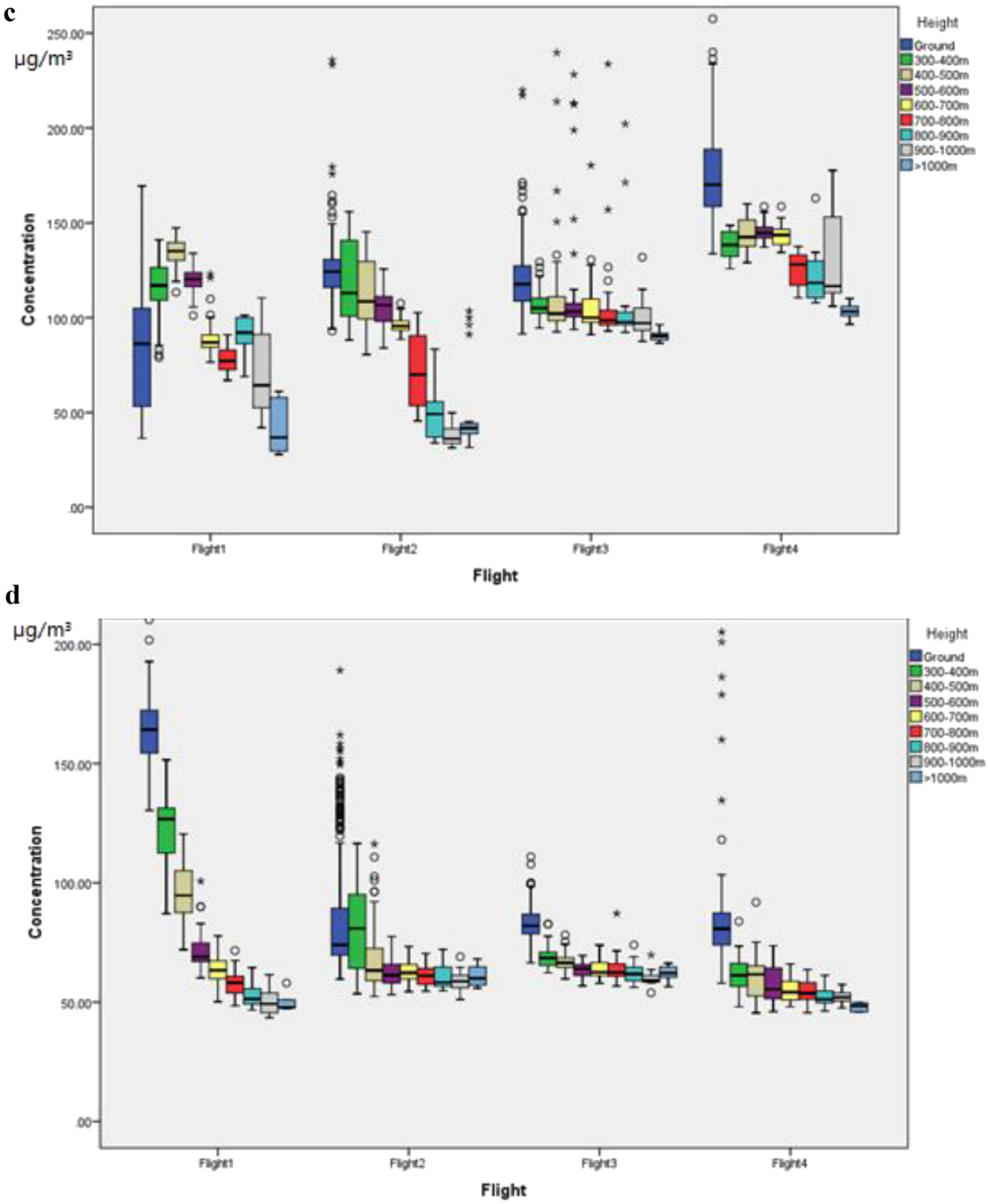


**Fig. 3.** (*continued*).

trapping the particle matters could explain this stratification. This is consistent with the study in Inn Valley (Harnisch et al., 2009). In the late morning, when stability of the atmosphere increased, vertical transport of particle matters may occur. This contributes to the mixing of pollutant in the altitude. As a result, the vertical gradient of the $PM_{2.5}$ concentration decrease. However, shallow inversion

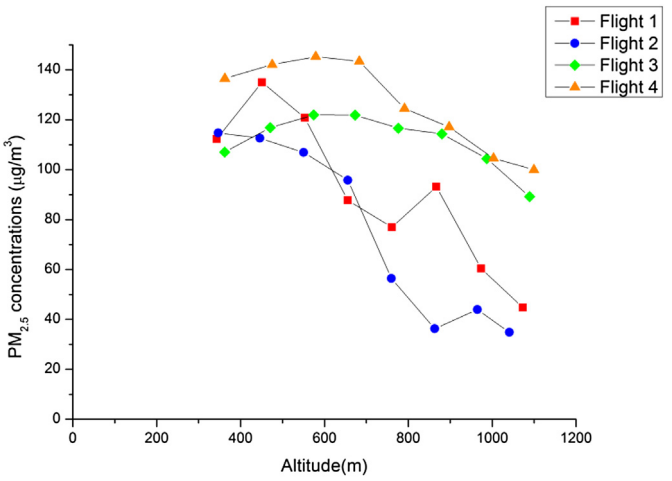


**Fig. 4.** $PM_{2.5}$ concentration changes with the increase of altitude on November 14th.

layer at 600 m altitude seems to prevail throughout the day, blocking an effective vertical exchange of the polluted air mass. As a result, positive vertical gradient are presented below 600 m altitude in the Flight 3 and 4.

### 3.2. The relationship between meteorological condition and $PM_{2.5}$ concentrations

#### 3.2.1. Correlation analysis

Meteorological condition's effect on dilution, diffusion and accumulation of pollutants has been universally recognized. We first use the correlation coefficient to analyze the relationship since Pearson correlation coefficient can reflect the linear correlation between two variables. Through the Pearson correlation analysis of the data, the strength of correlation between the independent variables and dependent variables can be determined. This paper selects the temperature, relative humidity, air pressure and height as independent variables, ratio of $PM_{2.5}$ concentration at different altitude above ground and near surface (F/G) as the dependent variable. The wind speed and wind direction are important variables that affect $PM_{2.5}$ concentration distributions, but are not considered in this analysis, because the wind speed and wind direction instruments could not be carried by the UAV. Besides, even if the instruments are put on the monitoring platform, it's really difficult to directly measure the actual wind speed and wind direction due to the turbulence caused by the movement of UAV. This is indeed the limitation of this analysis. Fortunately, the wind during the experiment days was not that strong judging from the ground weather station that we used.

The Pearson correlation coefficients among the observed parameters are calculated and the results are shown in Table 1a and b.

Pearson correlation analysis shows that independent variables temperature, relative humidity, air pressure and height have a high correlation with the dependent variable F/G. Temperature has the highest correlation with the F/G variable, with the correlation coefficients of 0.807, 0.895 and 0.762 during Flights 1, 2 and 3, respectively. However, during Flight 4, air pressure has the highest correlation with the F/G variable. What' more, as we can see, the variables temperature and air pressure always stay positive and variable height is negatively correlated with the dependent variable. It is noted that variable RH stays positive correlation during the first two flights in the morning while it changes into negative correlation during the last two flights in the afternoon. As is shown in Table 2a, RH has a strong relationship with Temperature with the correlation coefficient of 0.855, while air pressure has even higher relevance to Height with the correlation coefficient of 0.986. Table 2b.

**Table 1a**
Pearson correlation coefficient between independent and dependent variable (based on data on August 21st).

| | Temperature | RH | Air pressure | Height |
|---|---|---|---|---|
| F1/G1 | **0.807** | 0.742 | 0.754 | −0.759 |
| F2/G2 | **0.895** | 0.867 | 0.875 | −0.886 |
| F3/G3 | **0.762** | −0.674 | 0.738 | −0.742 |
| F4/G4 | 0.706 | −0.662 | **0.739** | −0.734 |

F1/G1, F2/G2, F3/G3 and F4/G4 refer to ratio of $PM_{2.5}$ concentration at different altitude above ground and near surface during Flights 1, 2, 3 and 4, respectively. (The most influential factors are highlighted in bold.)

**Table 1b**
Pearson correlation coefficient between independent and dependent variable (based on data on October 11th).

| | Temperature | RH | Air pressure | Height |
|---|---|---|---|---|
| F1/G1 | **0.799** | 0.643 | 0.783 | −0.698 |
| F2/G2 | 0.634 | **0.823** | 0.798 | −0.832 |
| F3/G3 | 0.779 | −0.735 | **0.814** | −0.684 |
| F4/G4 | **0.786** | −0.582 | 0.765 | −0.712 |

The bold factors are the most influential factors (with the largest absolute value in the same flight).

#### 3.2.2. Normality test

In order to test for normality of the dependent variables, we test the distribution of variables' residual error. Results expressed as a histogram as shown in Fig. 5. From the histogram it can be drawn, residual error $\varepsilon$ is fitted to the normal distribution, and it satisfies the normal distribution requirement of the regression model (mean $= 0$, variance $= \sigma^2$)

#### 3.2.3. Model development and results

The normality test and correlation analysis show that the conditions of multiple regression are met. Therefore, before using the multiple linear regression method to model the vertical distribution of $PM_{2.5}$, we need to take the autocorrelation of the parameters since the observed data is closely related with time. The autocorrelation in the dataset is tested with the Durbin–Watson test.

*DW* values of four flights are 0.760, 1.612, 1.597 and 1.479. Therefore, it indicates that there is no autocorrelation problem in the regression model for Flights 2–4, but there may be an

**Table 2a**
Pearson correlation coefficients of independent variables (on August 21st).

| | Temperature | RH | Air pressure | Height |
|---|---|---|---|---|
| Temperature | – | **0.855** | 0.038 | 0.171 |
| RH | | – | −0.062 | 0.062 |
| Air pressure | | | – | **0.986** |
| Height | | | | – |

**Table 2b**
Pearson correlation coefficients of independent variables (on October 11th).

| | Temperature | RH | Air pressure | Height |
|---|---|---|---|---|
| Temperature | – | **0.912** | 0.016 | **0.793** |
| RH | | – | −0.056 | 0.102 |
| Air pressure | | | – | **0.874** |
| Height | | | | – |

The relationships of high correlation are highlighted in bold.

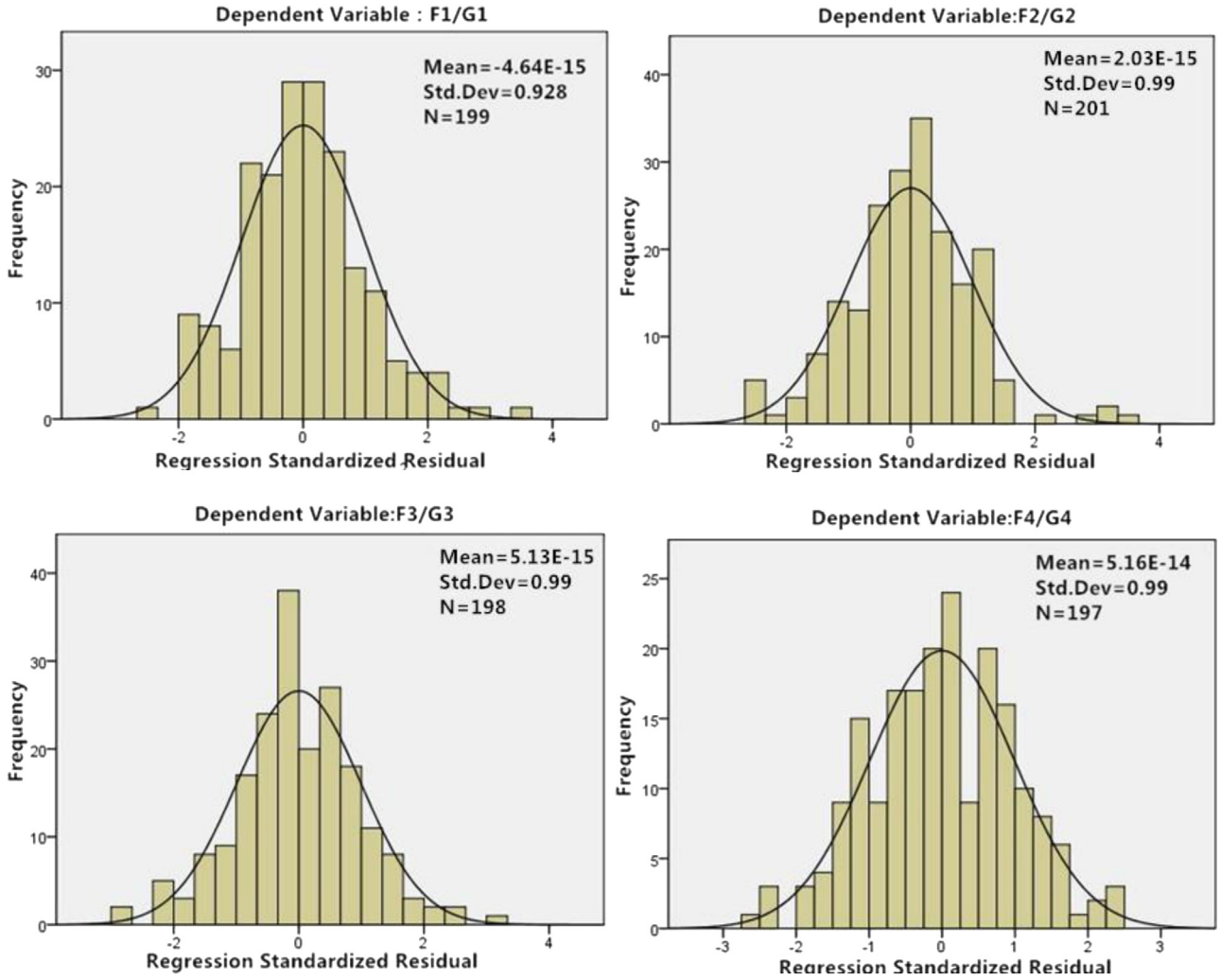


**Fig. 5.** Standardized residual histogram.

autocorrelation problem for Flight 1.

Considering the high value in Pearson's Correlation analysis and that multicollinearity may cause great influence to the validity of the multiple linear regression model, stepwise regression is used in this paper to avoid the multicollinearity issue. In stepwise regression, factors are added into the model one by one, and the factor that may cause multicollinearity problem will not be added into the model. Tables 3a and b shows the stepwise regression result.

As is shown in Tables 3a and b, results of all the four flights have

**Table 3a**
Stepwise multiple linear regression result (on August 21st).

| | Temperature | RH | Air pressure | Altitude | Constant | $R^2$ | DW | F |
|---|---|---|---|---|---|---|---|---|
| Flight 1 | 9.873[a] | 8.428[a] | 7.318[a] | 0.003 | −11.087[a] | 0.581 | 0.460 | 232.534 |
| Flight 2 | 10.139[a] | 10.746[a] | 0.115 | 1.075[b] | −5.26[a] | 0.776 | 0.932 | 375.229 |
| Flight 3 | 8.23[a] | 2.015 | −1.84[b] | – | −0.79[a] | 0.593 | 1.365 | 158.905 |
| Flight 4 | 5.011[a] | −1.020 | – | – | −8.036[a] | 0.489 | 1.069 | 183.347 |

**Table 3b**
Stepwise multiple linear regression result (on October 11th).

| | Temperature | RH | Air pressure | Altitude | Constant | R2 | DW | F |
|---|---|---|---|---|---|---|---|---|
| Flight 1 | 10.907[a] | 8.841[a] | 6.953[a] | – | −10.84[a] | 0.751 | 0.760 | 189.410 |
| Flight 2 | 10.863[a] | 11.722[a] | 1.994[b] | 1.15[a] | −5.308[a] | 0.886 | 1.612 | 389.275 |
| Flight 3 | 6.24[a] | 4.361[a] | −1.98[b] | – | −0.85[b] | 0.691 | 1.597 | 107.811 |
| Flight 4 | 5.551[a] | −3.000[a] | – | – | −6.076[a] | 0.563 | 1.479 | 127.267 |

[a] Indicates significant at 99% level of confidence.
[b] Indicates significant at 95% level of confidence.

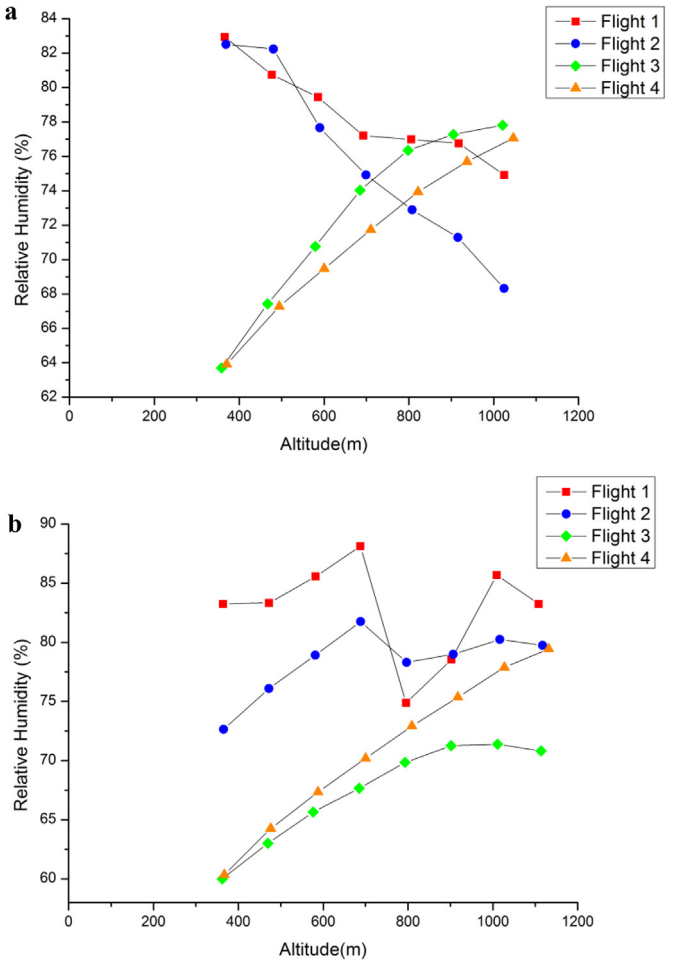


**Fig. 6.** a. Vertical profiles of relative humidity during four flights on August 21st. b. Vertical profiles of relative humidity during four flights on October 11th.

relatively high R-square values, indicating a relatively good fit of the model to the observed data, with the more flights (Flights 1–2) fit better than the afternoon flights (Flights 3–4). It can also be seen that the results are very much similar for the two days' of observation data on August 21st and October 11th, 2014.

### 3.2.4. *The impact of temperature and relative humidity on vertical distributions of $PM_{2.5}$ concentration*

These modeling results indicate that temperature has close association with relative $PM_{2.5}$ concentration (*F/G*). Comparing different flights, the coefficients of temperature go down from 10.907 to 5.551 for Flights 1 to 4, indicating that the influence of temperature on $PM_{2.5}$ concentration decreases with time during the day. At about 6:00–7:30 in the morning (Flight 1), the influence of temperature is the highest.

The vertical distribution of air temperature reflects the stability of the atmospheric structure which impacts the strength of turbulence activity, and governs the spread of air pollution. Through the discussion above, it is concluded that the diurnal variation of air temperature has significant effect on the vertical $PM_{2.5}$ concentration distribution within the range from 300 m to 1000 m off the ground.

Similarly, as is discussed in Section 3.2.3, the influence of relative humidity towards $PM_{2.5}$ concentration is significant during the daytime. However, the coefficient of *RH* in the regression model is higher in the morning than that in the afternoon. This may be due to the higher relative humidity in the morning than in the afternoon (Fig. 6a and b). Also, the relative humidity decreases as height increases in the morning. Based on the meteorological data recorded by weather bureau of Hangzhou, weather condition around the experiment date is shown in Table 4. The clouds dispersed in the morning and the sun radiation increases. What's more, the atmospheric humidity decreases gradually so that the influence of humidity on $PM_{2.5}$ concentration level is reduced.

**Table 4**
Weather condition in August, 2014, in Hangzhou.

| | 18th | 19th | 20th | 21th |
|---|---|---|---|---|
| Weather | Rainy | Rainy | Cloudy | Cloudy to Sunny |

### 3.2.5. *The impact of thermal inversion on vertical profile of $PM_{2.5}$ concentration*

Fig. 6a and b shows the vertical profiles of temperature during four flights. It can be seen that temperature generally decreases as height increases. However, the only exception takes place in Flight 1 between 300 m and 500 m that shows temperature inversion on August 21st. This thermal inversion layer may be responsible for the inversion of $PM_{2.5}$ concentrations at that altitude, because the thermal inversion obstructs the vertical movements of the airflow.

The thermal inversion is formed due to the heterogeneity of terrain and underlying surface and meteorological conditions, which could produce dynamic and thermodynamic effects towards airflow movements and change the spread condition to air pollutant (e.g., urban heat island phenomena). In addition, the weather is clear and wind speed is small (on August 21, the detection of wind speed <3 kts), accompanied by the air sinking movement, subsidence inversion formed at a few hundred meters' or higher altitude, suppressing turbulence to develop.

To take into account the effects of the temperature inversion, we introduce a dummy variable to describe the influence of thermal inversion to $PM_{2.5}$ concentration distribution. The monitoring data on August 21st are used for this analysis.

$$\mathrm{D.V} = \begin{cases} 0 & t_{i+1} - t_i \le 0 \\ 1 & t_{i+1} - t_i > 0 \end{cases} \quad (2)$$

where *D.V* is dummy variable, *t* is temperature.

As thermal inversion exists during Flight 1 (Fig. 7a), the data recorded during Flight 1 are used to compare the results before and after adding the dummy variable (Table 5).

As it is shown, the $R^2$ of the regression model improves after the dummy variable *D.V* is added. The autocorrelation issue disappeared as well after adding the dummy variable. The results show at the thermal inversion layer, temperature become more important in affecting the $PM_{2.5}$ concentration than the layer above it, with the coefficient of 26.75 (= 12.268 + 14.482) at the thermal inversion layer and 10.843 above it. Furthermore, the altitude variable at the thermal inversion layer is no longer significant, further indicating the dominant importance of temperature in affecting the $PM_{2.5}$ concentration.

### 3.3. *Multiple regression model for modeling vertical distribution of $PM_{2.5}$*

As the multiple linear regression models on August and October have different coefficients, we use data measured in four months (August, October, November and December) to form a general model. Thus, dummy variables, isFlight1, isBelow and isThermal,

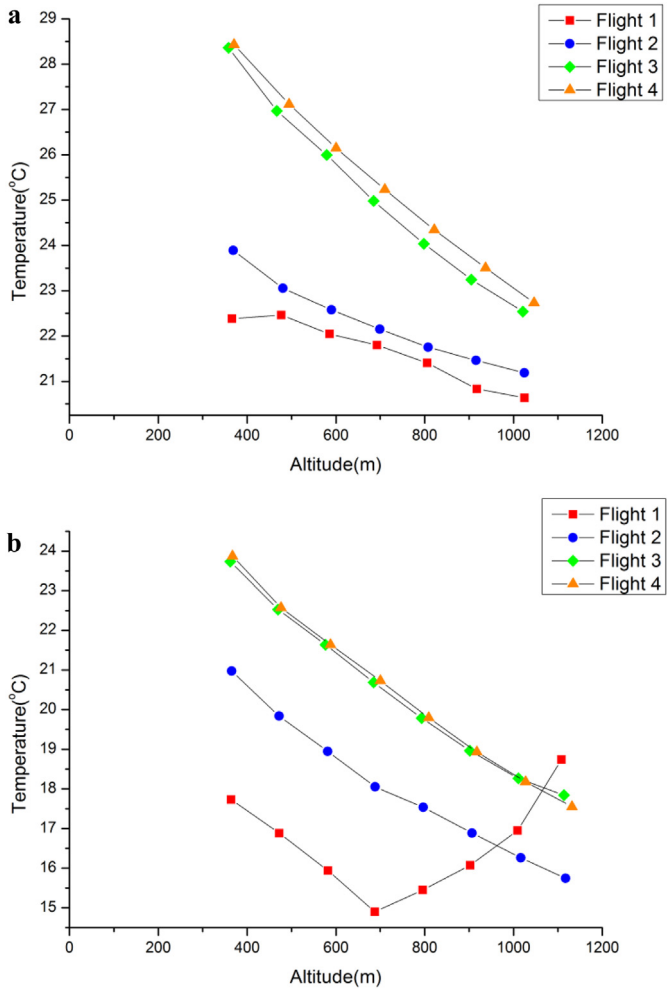


**Fig. 7.** a. Vertical profiles of temperature during four flights on August 21st. b. Vertical profiles of temperature during four flights on October 11th.

have been introduced to improve the multiple regression model. Dummy variable isFlight1 shows that the vertical distribution pattern in Flight 1 is different from the other three flights, as a result, the coefficients of RH and temperature in Flight 1 are quite different from those in Flight 2, 3 and 4. Dummy variable isBelow represents the atmospheric boundary layer has a significant effect on the vertical distribution. Dummy variable isThermal illustrates that thermal inversion layers limit the vertical transportation of the particle matter causing the positive vertical gradient within it, while negative vertical gradient outside it. These three dummy variables are designed as below:

$$isFlight1 = \begin{cases} 1, & during\ Flight1 \\ 0, & otherwise \end{cases} \quad (3)$$

**Table 6**
The coefficients of the new multiple regression model.

| | a | b | c | d |
|---|---|---|---|---|
| 1 | 1.0439 | – | – | −0.0004 |
| 2 | 2.4347 | 0.2201 | −0.0443 | −0.0024 |
| 3 | 1.5402 | 0.0400 | −0.0424 | 0.001 |
| 4 | – | 0.0349 | −0.0141 | 0.0008 |

$$isBelow = \begin{cases} 1, & below\ thermal\ inversion\ layer \\ 0, & otherwise \end{cases} \quad (4)$$

$$isThermal = \begin{cases} 1, & in\ thermal\ inversion\ layer \\ 0, & otherwise \end{cases} \quad (5)$$

In this general multiple regression, variables Temp, RH and Altitude are supposed to explain the meteorological factors and dummy variables isFlight1, isBelow and isThermal are used to explain the PBL and inversion layer effect. The model is shown as below:

$$\begin{aligned} F/G = {} & (a1 + b1{*}Temp + c1{*}RH + d1{*}Altitude) + isFlight1{*}(a2 \\ & + b2{*}Temp + c2{*}RH + d2{*}Altitude) + isBelow{*}(a3 \\ & + b3{*}Temp + c3{*}RH + d3{*}Altitude) + isThermal{*}(a4 \\ & + b4{*}Temp + c4{*}RH + d4{*}Altitude) \end{aligned} \quad (6)$$

Table 6 shows the result of the new multiple regression model; and R-square is 0.704, indicating a relatively good fit of the model to the observed data. Generally, relative $PM_{2.5}$ concentration increases when temperature goes up, and decreases when relative humidity goes up because the value of coefficient b is positive while c is negative. This pattern is similar to the results in Table 3a and b.

In addition, relative $PM_{2.5}$ concentration ($F/G$) decreases as altitude goes up since d1 and d2 are negative (see Table 6) and the sum of the d row is negative. In the early morning (during Flight 1), relative $PM_{2.5}$ concentration goes down faster by altitude because d2 is smaller than d1. But for data below or in thermal inversion layer, $F/G$ may increase with altitude going up as d3 and d4 are positive.

When particle matter is located below or in thermal inversion layer, temperature and relative humidity are more important because the absolute value of b and c is greater than c. During Flight 1 when isFlight1 equals 1, temperature has the most important influence since b2 equals 0.2201 which is bigger than b3 and b4.

## 4. Conclusions

In this study, UAV equipped with mobile monitoring devices was used for collecting $PM_{2.5}$ mass concentration data within altitude of 1000 m in a 4 km*4 km area in Lin'an, a suburb of Hangzhou city, China. The study demonstrates the feasibility of UAV with mobile monitoring devices as an effective and flexible means to collect three-dimensional air pollutant concentration data, particularly for monitoring the vertical profile of air pollutants.

**Table 5**
Comparison of regression result of Flight 1 with or without adding *D.V*.

| | Temp | RH | Pressure | Altitude | D.V | Constant | $R^2$ | DW |
|---|---|---|---|---|---|---|---|---|
| Without | 10.843[a] | 8.841[a] | – | 6.953[a] | | −10.841 | 0.751 | 0.760 |
| With | 12.268[a] | 13.649[a] | – | – | 14.482[a] | −29.864 | 0.853 | 1.353 |

[a] indicates significant at the 1% level.

This study found that $PM_{2.5}$ concentrations generally decrease as altitude increases, with the exception of the thermal inversion layer. $PM_{2.5}$ concentrations also change during the day, and present an increasing trend from the morning to the afternoon. The variations of vertical profiles are different between morning and afternoon, but there are similar vertical patterns between two flights in the morning or in the afternoon. In particular, there is no significant difference from 2:00pm to 5:00pm because the air has been thoroughly mixed within 1000 m of the atmospheric boundary layer. The vertical profile of the $PM_{2.5}$ concentrations is also influenced by meteorological parameters (i.e., air temperature, relative humidity and air pressure) and height from 300 m to 1000 m above the ground. Air temperature has the most important effect on the vertical variation of $PM_{2.5}$ concentrations. Additionally, relative humidity significantly affects the vertical profile of $PM_{2.5}$ concentrations. Both air temperature and relative humidity have more significant effects on the vertical pattern of $PM_{2.5}$ concentrations in the morning than that in the afternoon. This finding is consistent for two-days of flights in August and October, indicating some consistency in our findings. But more experiments and data are needed to generalize the vertical patterns of $PM_{2.5}$ distribution during the day and different seasons.

A general multiple regression model with dummy variables is developed to illustrate both meteorological parameters and atmospheric stratification effect. This regression describes the $PM_{2.5}$ temporal and spatial distribution well and its R-square equals 0.704. What's more, the model emphasizes the atmospheric boundary layer's and thermal inversion layer's influence on the $PM_{2.5}$ vertical distribution. When the atmospheric boundary layer height is low (in Flight 1), the particulate matter was limited in the atmospheric boundary layer contributing to relative $PM_{2.5}$ concentration going down faster by altitude than when the atmospheric boundary layer uplift later in the day. The coefficients show that altitude is the most important factor, except for Flight 1 when temperature has the highest coefficients. But if considering thermal inversion layer, temperature and relative humidity are more important.

Through this study, it demonstrates the potential of an innovative technology of unmanned aerial vehicle (UAV) equipped with mobile sensors to observe three-dimensional air pollutant concentrations. However, there are still limitations to be improved in the future. For example, four day's data are not adequate to find different patterns with varied seasons or under varied weather conditions. Moreover, sixteen flights' data in four days seem not enough to accurately describe the vertical distribution pattern during the day either, particularly in the night where temperature and the atmospheric boundary layer are lower. Therefore, more experiments in different seasons with various weather conditions and under different pollution events (e.g., heavy smog conditions) should be conducted to fully understand the vertical distribution patterns of different pollutants in different meteorological conditions.

## Acknowledgment

This study is supported by Scientific Project of Shanghai Environmental Protection Bureau (No. 2014-8), Science Technology Department of Zhejiang Province (2014C31028), and the State Key Laboratory of Ocean Engineering of China (GKZD010059) at Shanghai Jiao Tong University. We express appreciation for the Second Surveying and Mapping Institute of Zhejiang Province for cooperation in flying the UAV for the experiments. We also wish to acknowledge the support from the Shanghai Environmental Monitoring Center for assistance in the instrumental calibration process. Finally, we would like to thank graduate students Hongwei Wang, Cong Bai, Xiaobing Li, Wenzhuo Lu from the Center for ITS and UAV Applications Research at Shanghai Jiao Tong University for their help in data collection.

## References

Altstädter, B., Platis, A., Wehner, B., Scholtz, A., Wildmann, N., Hermann, M., , et al.Lampert, A., 2015. ALADINA—an unmanned research aircraft for observing vertical and horizontal distributions of ultrafine particles within the atmospheric boundary layer. Atmos. Meas. Tech. 8 (4), 1627–1639.

Berkes, F., Hoor, P., Bozem, H., Weigel, R., Wendling, J., Meixner, F.X., Sprenger, M., Lelieveld, J., 2013. Case study: aircraft-based observation of vertical mixing event in the lower atmosphere during PARADE 2011. EGU General Assembly Conf. Abstr. 15, 11673.

Chang, D., Song, Y., Liu, B., 2009. Visibility trends in six megacities in China 1973-2007. Atmos. Res. 94 (2), 161–167.

Che, H.Z., Zhang, X.Y., Li, Y., et al., 2009. Haze trends over the capital cities of 31 provinces in China, 1981–2005. Theor. Appl. Climatol. 97, 235–242.

Chen, B.B., Sverdlik, L.G., Imashev, S.A., Solomon, P.A., Lantz, J., Schauer, J.J., Shafer, M.M., Artamonova, M.S., Carmichael, G.R., 2013a. Lidar measurements of the vertical distribution of aerosol optical and physical properties over Central Asia. Int. J. Atmos. Sci. 2013.

Chen, P., Zhang, Q., Quan, J., Gao, Y., Zhao, D., Meng, J., 2013b. Ground-high altitude joint detection of ozone and nitrogen oxides in urban areas of Beijing. J. Environ. Sci. 25 (4), 758–769.

Corrigan, C.E., Roberts, G.C., Ramana, M.V., Kim, D., Ramanathan, V., 2008. Capturing vertical profiles of aerosols and black carbon over the Indian Ocean using autonomous unmanned aerial vehicles. Atmos. Chem. Phys. 8 (3), 737–747.

Day, D.E., Malm, W.C., Kreidenweis, S.M., 2000. Aerosol light scattering measurments as a function of relative humidity. J. Air Waste Manag. Assoc. 50, 710–716.

Fu, X., Wang, S., Zhao, B., Xing, J., Cheng, Z., Liu, H., Hao, J., 2013. Emission inventory of primary pollutants and chemical speciation in 2010 for the Yangtze River Delta region, China. Atmos. Environ. 70, 39–50.

Geng, F., Zhang, Q., Tie, X., Huang, M., Ma, X., Deng, Z., Yu, Q., Quan, J., Zhao, C., 2009. Aircraft measurements of O3, NOx, CO, VOCs, and SO2 in the Yangtze River Delta region. Atmos. Environ. 43 (3), 584–593.

Han, S., Bian, H., Tie, X., Xie, Y., Sun, M., Liu, A., 2009. Impact of nocturnal planetary boundary layer on urban air pollutants: measurements from a 250-m tower over Tianjin, China. J. Hazard. Mater. 162 (1), 264–269.

Harnisch, F., Gohm, A., Fix, A., Schnitzhofer, R., Hansel, A., Neininger, B., 2009. Spatial distribution of aerosols in the Inn Valley atmosphere during wintertime. Meteorol. Atmos. Phys. 103 (1–4), 223–235.

Li, C., Krotkov, N.A., Dickerson, R.R., Li, Z., Yang, K., Chin, M., 2010. Transport and evolution of a pollution plume from northern China: a satellite-based case study. J. Geophys. Res. 115, D00K03. http://dx.doi.org/10.1029/2009JD012245.

Ma, Z., Hu, X., Sayer, A.M., Levy, R., Zhang, Q., Xue, Y., Tong, S., Bi, J., Huang, L., Liu, Y., 2015. Satellite-based spatiotemporal trends in PM2. 5 concentrations: China, 2004–2013. Environ. Health Perspect. http://dx.doi.org/10.1289/ehp.1409481.

McMurry, P.H., Zhang, X., Lee, C.T., 1996. Issues in aerosol measurement for optics assessments. J. Geophys. Res. Atmos. 1984–2012 101 (D14), 19189–19197.

Nunnermacker, L.J., Weinstein-Lloyd, J.B., Hillery, B., Giebel, B., Kleinman, L.I., Springston, S.R., Daum, P.H., Gaffney, J., Marley, N., Huey, G., 2008. Aircraft and ground-based measurements of hydroperoxides during the 2006 MILAGRO field campaign. Atmos. Chem. Phys. 8, 7619–7636.

Ou-Yang, C.F., Lin, N.H., Lin, C.C., Wang, S.H., Sheu, G.R., Lee, C.T., Schnell, R.C., Lang, P.M., Kawasato, T., Wang, J.L., 2014. Characteristics of atmospheric carbon monoxide at a high-mountain background station in East Asia. Atmos. Environ. 89, 613–622.

Quan, J., Zhang, Q., He, H., et al., 2011. Analysis of the formation of fog and haze in North China Plain (NCP). Atmos. Chem. Phys. 11 (15), 8205–8214.

Raatikainen, T., Hyvärinen, A.P., Hatakka, J., Panwar, T.S., Hooda, R.K., Sharma, V.P., Lihavainen, H., 2014. The effect of boundary layer dynamics on aerosol properties at the Indo-gangetic plains and at the foothills of the Himalayas. Atmos. Environ. 89, 548–555.

Ramana, M.V., Ramanathan, V., et al., 2007. Albedo, atmospheric solar absorption and heating rate measurements with stacked UAVs. Q. J. R. Meteorol. Soc. 133, 1913–1931.

Ramanathan, V., Ramana, M.V., Roberts, G., Kim, D., Corrigan, C., Chung, C., Winker, D., 2007. Warming trends in Asia amplified by brown cloud solar absorption. Nature 448 (7153), 575–578.

Ramanathan, V., Carmichael, G., 2008. Global and regional climate changes due to black carbon. Nat. Geosci. 221–227.

Ramanathan, V., Feng, Y., 2009. Air pollution, greenhouse gases and climate change: Global and regional perspectives. Atmos. Environ. 43, 37–50.

Sun, Y., Wang, Y., Zhang, C., 2009. Measurement of the vertical profile of atmospheric SO2 during the heating period in Beijing on days of high air pollution. Atmos. Environ. 43, 468–472.

Streets, D.G., Canty, T., Carmichael, G.R., de Foy, B., Dickerson, R.R., Duncan, B.N., Edwards, D.P., Haynes, J.A., Henze, D.K., Houyoux, M.R., Jacob, D.J., Krotkov, N.A., Lamsal, L.N., Liu, Y., Lu, Z., Martin, R.V., Pfister, G.G., Pinder, R.W., Salawitch, R.J., Wecht, K.J., 2013. Emissions estimation from satellite retrievals: a review of current capability. Atmos. Environ. 77, 1011–1042.

Stull, R.B., 1988. An Introduction to Boundary Layer Meteorology[M]. Springer.
Taubman, B.F., Hains, J.C., Thompson, A.M., Marufu, L.T., Doddridge, B.G., Stehr, J.W., Piety, C.A., Dickerson, R.R., 2006. Aircraft vertical profiles of trace gas and aerosol pollution over the mid-Atlantic United States: Statistics and meteorological cluster analysis. J. Geophys. Res. Atmos. (1984–2012) 111 (D10).
Wang, H., Tan, S.C., Wang, Y., Jiang, C., Shi, G.Y., Zhang, M.X., Che, H.Z., 2014. A multisource observation study of the severe prolonged regional haze episode over eastern China in January 2013. Atmos. Environ. 89, 807–815.
Wang, Z., Lu, F., He, H.D., Lu, Q.C., Wang, D., Peng, Z.R., 2015a. Fine-scale estimation of carbon monoxide and fine particulate matter concentrations in proximity to a road intersection by using wavelet neural network with genetic algorithm. Atmos. Environ. 104, 264–272.
Wöhrnschimmel, H., Márquez, C., Mugica, V., Stahel, W.A., Staehelin, J., Cárdenas, B., Blanco, S., 2006. Vertical profiles and receptor modeling of volatile organic compounds over Southeastern Mexico City. Atmos. Environ. 40 (27), 5125–5136.
Wang, Z., He, H.D., Lu, F., Lu, Q.C., Peng, Z.R., 2015b. Hybrid model for prediction of carbon monoxide and fine particulate matter concentrations near a road intersection. Transp. Res. Rec. J. Transp. Res. Board 2503, 29–38.
Zhang, Q., He, K.B., Huo, H., 2012. Cleaning China's air. Nature 484, 161–162.